Role of Interstitial Apatite Plaque in the Pathogenesis of the Common Calcium Oxalate Stone

Andrew P. Evan, PhD, James E. Lingeman, MD,† Fredric L. Coe, MD,‡ and Elaine M. Worcester, MD‡*

Summary: By using intraoperative papillary biopsy material from kidneys of idiopathic calcium oxalate, intestinal bypass for obesity, brushite, cystine, and distal renal tubular acidosis stone formers during percutaneous nephrolithotomy, we have determined that idiopathic calcium oxalate stone formers appear to be the special case, although the most commonly encountered one, in which stones form external to the kidney and by processes that do not involve the epithelial compartments. It is in this one group of patients that we find not only abundant interstitial plaque, but also strong evidence that the plaque is essential to stone formation. The initial site of plaque formation is always in the papillary tip, and must be in the basement membrane of the thin loop of Henle. With time, plaque spreads throughout the papilla tip to the urothelium, which under conditions we do not understand is denuded and thereby exposes the apatite deposits to the urine. It is on this exposed apatite that a stone forms as an overgrowth, first of amorphous apatite and then layers of calcium oxalate. This process generates an attached stone fixed to the side of a papilla, allowing the ever-changing urine to dictate stone growth and composition.

Semin Nephrol 28:111-119

Keywords: *Loops of Henle, papillary biopsies, hyaluronan*

Above all, one can say that stone disease is various. Stones can be composed of calcium oxalate (CaOx), calcium phosphate including apatite and brushite, uric acid, cystine, struvite, drugs, and a host of minor and rare crystals.[1] Within many of these stone groups the causes, proven or suspected, run on to lists of diseases, traits, urine chemistry abnormalities, and diet patterns, so stones can best be called the end product of innumerable causes. Here we are interested in the most common type of stone patient, one whose stones are predominantly on average greater than 50% CaOx and in whom one can exclude with confidence all of the systemic diseases known to cause such stones. These patients often are called *idiopathic calcium stone formers* (ICSFs), although most if not all harbor the genetic trait of hypercalciuria, not so much a disease as one tail of the distribution of urine calcium excretions found in human beings.[1] It is in this one group of patients that we find not only abundant interstitial plaque, but also strong evidence that the plaque is essential to stone formation.

ORIGIN OF PLAQUE

The initial site of plaque formation is always in the papillary tip, and must be in the basement membrane of the thin loop of Henle[2] because that is the one site always involved with plaque when any plaque is present, and it is the only site involved with plaque in isolation (Fig. 1A). Within the basement membrane plaque are in-

*Department of Anatomy and Cell Biology, Indiana University School of Medicine, Indianapolis, IN.
†Methodist Hospital Institute for Kidney Stone Disease, Indianapolis, IN.
‡Nephrology Section, University of Chicago, Chicago, IL.
Supported in part by National Institutes of Health grant PO1 DK56788.
Address reprint requests to Andrew P. Evan, PhD, Chancellor's Professor, Department of Anatomy and Cell Biology, Indiana University School of Medicine, 635 Barnhill Dr, MS5035, Indianapolis, IN 46202-5120. E-mail: evan@anatomy.iupui.ed
0270-9295/08/$ - see front matter
 doi:10.1016/j.semnephrol.2008.01.004

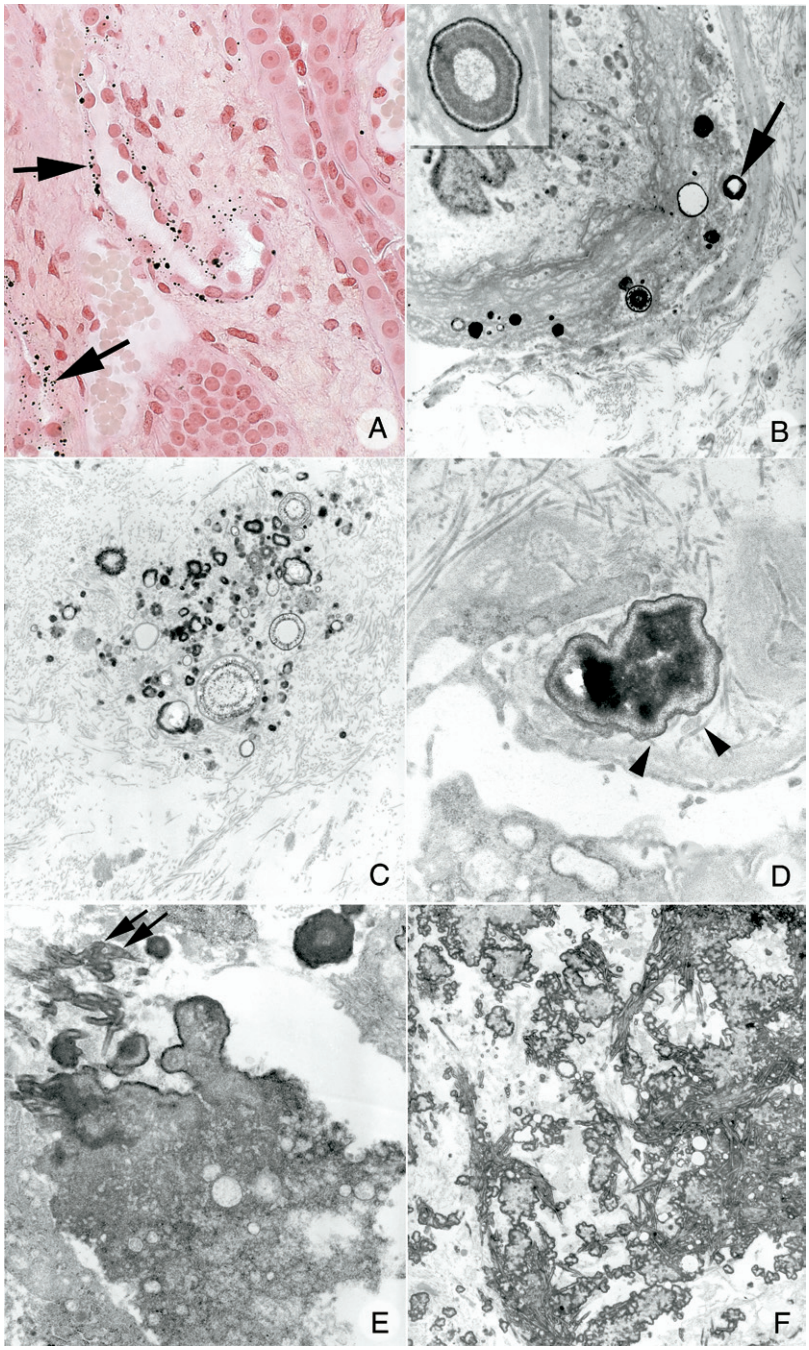

Figure 1. Initial sites of interstitial plaque and its progression. (A and B) The initial site of interstitial deposits (arrows) is the basement membranes of thin loops of Henle at the papilla tip as seen by (A) light and (B) transmission electron microscopy. (B) They appear as multilayered spheres (insert). (C and D) With time these deposits appear to migrate into the near interstitial space where they are associated with (D) type 1 collagen bundles (arrowheads). (E) These individual deposits coalesce (double arrows) to form (F) islands of mineral in an organic sea. Magnification is as follows: (A) 1,800×, (B and C) 30,000×, (D) 35,000×, (E) 30,000×, and (F) 23,000×.

dividual particles of alternating mineral and organic layers in a tree-ring configuration (Fig. 1B). Plaque clearly migrates from the basement membrane into the surrounding interstitium (Fig. 1C), and when it does so the individual particles can be found associated in an orderly way on type 1 collagen (Fig. 1D). Subsequently, particles associated with type 1 collagen fuse into a syncytium in which islands of mineral appear to float in an organic sea (Fig. 1E). We

believe this final form of plaque actually is composed of fused particles still in association with collagen, and that the plaque organic matrix, mineral, and collagen are associated tightly (Fig. 1F). As is evident in all panels of Figure 1, the mineral phase of plaque always is overlaid with organic matrix, so that uncoated mineral is never present.

COMPOSITION OF PLAQUE

The mineral phase of plaque invariably is biological apatite as determined by high-resolution Fourier transform infrared (FTIR) and electron diffraction.[2] Within plaque osteopontin (OP) is abundant (Fig. 2A). Within individual particles, OP localizes preferentially at the interface between the apatite and the adjacent organic matrix[3] (Fig. 2B). The third heavy chain (H3) of the inter-alpha trypsin molecule (ITI) is present in plaque[4] (Fig. 2C). Within individual particles, H3 localizes within the organic matrix layers (Fig. 2D), a site different from that of OP. H3 also is present in the interstitium, more abundant in ICSFs than in normals (Fig. 2C), and colocalizes with hyaluronin. OP is well known to slow the growth, aggregation, and nucleation of CaOx.[5-8] The ITI complex itself also is known to inhibit crystallization.[9-11] All molecules that affect crystallization tend to adhere to crystals, so the localization of OP at the mineral interface is not surprising. Whether H3 itself affects crystals is not known.

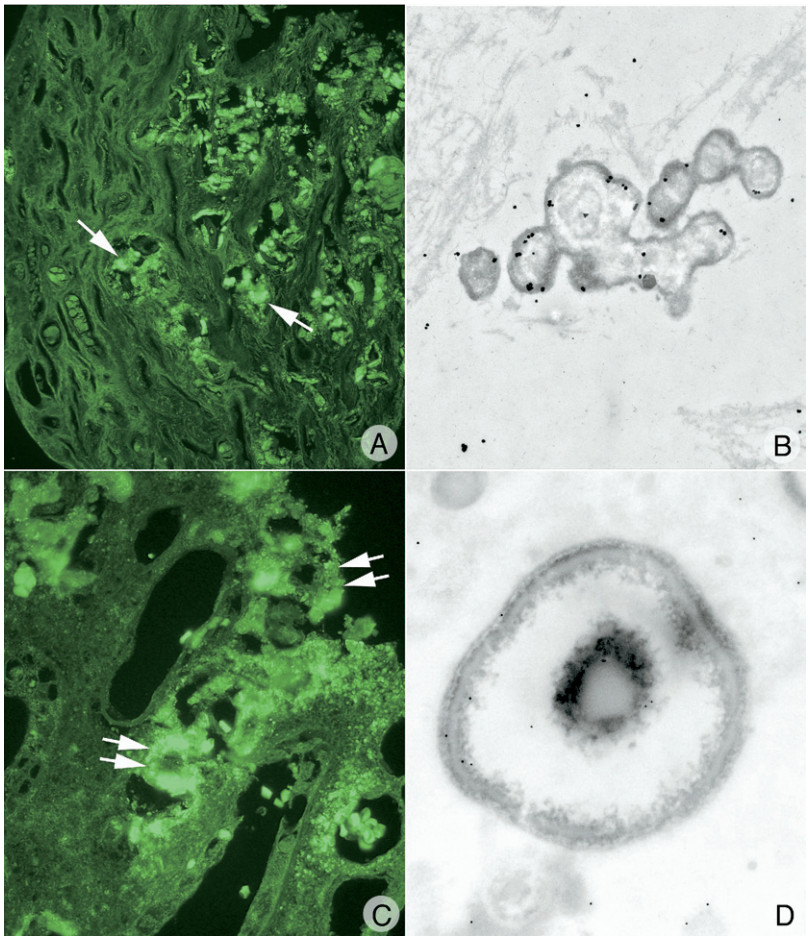

Figure 2. Immunohistochemical localization of osteopontin and ITI H3 in interstitial plaque. Both (A) OP (arrows) and (C) H3 of ITI (double arrows) are localized to the islands of interstitial plaque. However, within single deposits, (B) immunoelectron staining of OP was found at the interface of the crystalline material and the organic matrix (dark dots) and (D) H3 only in the matrix layer (dark dots). Magnification is as follows: (A) 100×, (B) 30,000×, (C) 130×, and (D) 40,000×.

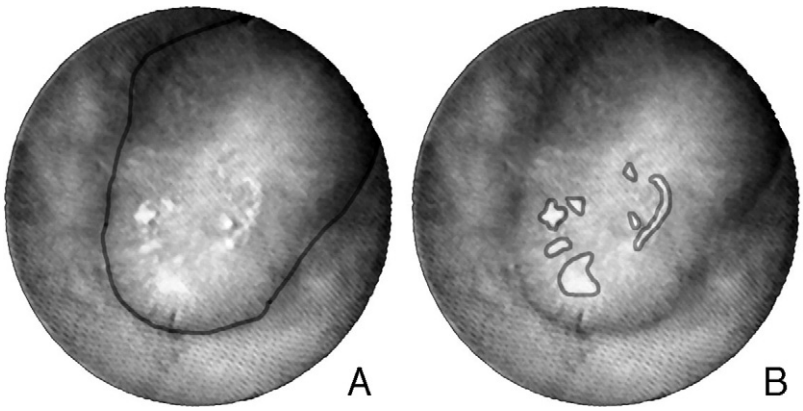

Figure 3. Digitized image of papillary plaque. (A) The papillary border was outlined to measure the total number of pixels encompassed within the papillary domain. (B) Next the individual sites of plaque were outlined so that the total pixel number could be measured within the plaque area domain. Reprinted with permission from Kuo et al.[12]

MECHANISMS FOSTERING PLAQUE

The abundance of plaque can be quantified using intraoperative digital imaging, and plaque is expressed as a percentage of coverage of the papillary surfaces[12] (Fig. 3). In patients for whom such quantification was performed, 24-hour urine samples collected at times random and remote from the surgery showed a strong positive correlation of plaque abundance with urine calcium excretion, and strong negative correlations with urine volume and pH (Fig. 4). Although we have no information about ion compositions in the interstitial microenvironment where plaque forms, these data suggest that high interstitial calcium concentrations are created by a combination of hypercalciuria and water conservation, and perhaps interstitial fluid pH is increased by urine acidification, lead-

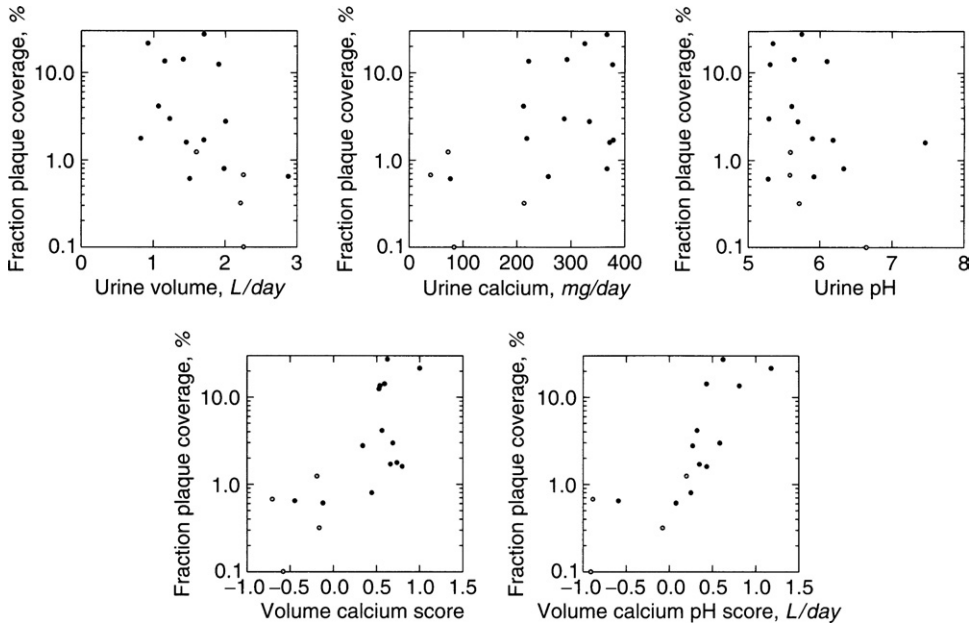

Figure 4. Urine correlates of papillary plaque. Fractional plaque coverage per papilium varies inversely with urine volume (upper left panel) among stone formers (●) and non–stone-forming control subjects (○). Plaque coverage varies with urine calcium excretion (upper middle panel) and is inverse to urine pH (upper right panel). A composite multivariate regression score using urine volume and calcium excretion (lower left panel) and one that includes urine pH as well (lower right panel) strongly correlates with plaque coverage. Reprinted with permission from Kuo et al.[12]

ing to formation of apatite in suitable matrix such as the thin limb basement membrane. How calcium might concentrate near the thin limbs is unknown, but the vas recta are very close to the limb so that their basement membranes are nearly in apposition, suggesting the vessels may be very important in the process.

EVIDENCE THAT CaOx STONES GROW ON PLAQUE

Perhaps the most obvious evidence is simple observation; CaOx stones are readily on plaque (Fig. 5A), from which they can be removed (Fig. 5B), leaving the original growth location bare (Fig. 5C). Others[13] have found evidence of plaque on stone surfaces. In a retrospective analysis of stone attachment, about 48% of stones were clearly on plaque at the time of removal; this figure is an underestimate because efforts were not made consistently to document the material to which stones were attached.[14] Clinical support comes from the fact that the number of stones formed, adjusted for the duration of stone disease, is proportional to the surface coverage by plaque,[15] what one would expect if plaque essentially were nucleating stones, or offering a secure lodging place for their growth.

MECHANISM FOR STONES TO GROW ON PLAQUE

En bloc biopsy of very small stones[16] permits us to show the anatomy and microstructure of the plaque–stone interface (Fig. 6A and B). Ultrastructure at the old attachment site (Fig. 7A) reveals a loss of urothelial cells; above the tissue, in the old urinary space, rafts of crystals (arrows) are imbedded in a homogeneous grey matrix accompanied by cell debris (arrowheads). Higher resolution of the region within the square (Fig. 7B) reveals that the exposed plaque is covered by a dark ribbon-like layer of alternating lamina of crystal (white in Figure

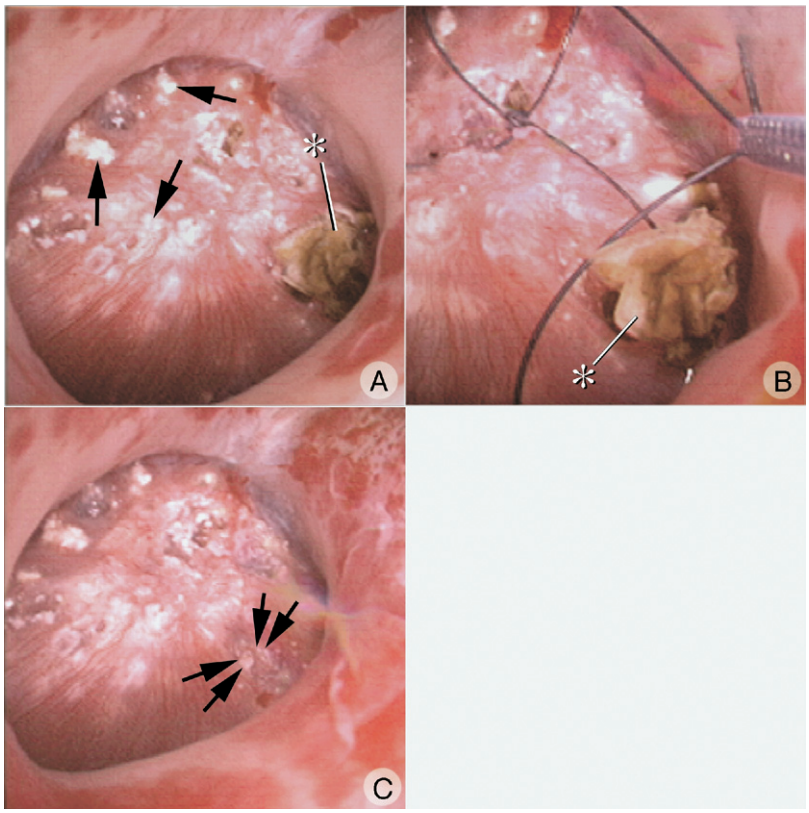

Figure 5. Digital image of a papilla from an ICSF patient obtained with an endoscope at the time of percutaneous nephrolithotomy. (A) Numerous sites of Randall's plaque (irregular white areas shown by arrows) as well as an attached stone (asterisk). (B) The stone is removed. (C) The same papilla after stone removal. This stone appears to have been attached to sites of Randall's plaque (double arrows).

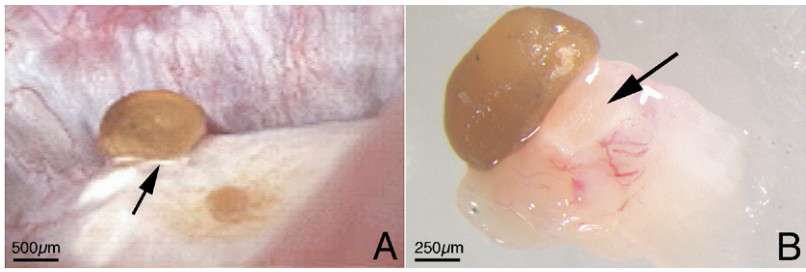

Figure 6. Human kidney stone. (A) Two stones adhere to a papillum of a CaOx stone former (patient 1, digital intraoperative endoscopic image). (B) During percutaneous nephrolithotomy the larger stone (arrow) was removed en bloc with its underlying tissue (light microscopy). (A) The edge of a region of Randall's plaque is visible just under the stone at the tip of the arrow. Reprinted with permission from Evan et al.[16]

7B) and black organic material (arrow). Crystals extend from the rafts into the outer surface of the ribbon (arrowheads). Higher resolution of the square (Fig. 7C) shows masses of tiny crystals growing directly in the outer ribbon (asterisk), the attachment site of one of the large raft crystals (arrows), and the crystals within the inner ribbon layers (visible in white). The blow-up inset shows the microcrystals within the inner lamina of the ribbon; one can count 4 white and 5 organic layers in this specimen. At the same resolution, at another location, one again sees the large raft crystals imbedded in their homogeneous matrix (double arrows) and masses of crystals growing in the outer layer of the ribbon (arrow).

On the stone itself one finds large rectangular crystals (arrows) at the interface similar to those in the raft (Fig. 8A). As one moves upward, into the bulk of the actual stone and away from the interface, these big crystals give way to masses of small crystals typical of stone architecture, and all imbedded in matrix (asterisk). The large crystals are in a matrix (Fig. 8B) that is quite different from plaque, it being more homogeneous (arrow) and lacking the large voids that plaque has because of its islands of apatite. At this magnification such islands would be larger than one of the large crystals.

This is not a movie, merely a single set of still pictures, but the sequence of events seems rather obvious. Plaque is exposed because urothelial cells either are damaged or undergo apoptosis; this step requires new research. After exposure the plaque is overlaid with new matrix. Tiny crystals form in the new matrix, in successive waves, forming the ribbons. At some point the rate and quantity of crystal formation permits explosive growth outward, so instead of lamina one finds heaping up of crystal into an anchored stone. This heaping up would extend the stone from the large initial crystals into the masses of smaller crystals as illustrated in Figure 8.

Evidence supports this sequence.[16] Another en bloc biopsy includes a stone so small it could be sectioned with only limited demineralization. Therefore, staining could identify crystals and permit outlining of the original interface (Fig. 9A, dotted white lines). FTIR spectra reveals biological apatite within plaque (Fig. 9B) as expected; at the interface itself (Fig. 9A, dotted lines) we found not biological apatite but an amorphous apatite (Fig. 9B). At area 1, the closest to the interface (Fig. 9, note both panels) we found biological apatite; at area 2, midway toward the stone periphery, we found a mixture of biological apatite and CaOx. At area 3, toward the periphery of the stone, we found pure CaOx. These findings are exactly what one would predict from the sequence proposed in the previously.

Immunohistochemistry reveals that OP is present in the stone and plaque, as expected, and crosses the interface without discontinuity.[16] Tamm–Horsfall protein, known to be restricted to the urine and thick ascending limb of the loop of Henle, is present only on the urine space side of the interface, and extends to the interface surface. From these findings we presume that the organic material forming the ribbon overlay on exposed plaque comes from urine molecules adsorbed initially onto the matrix of plaque. As new crystals nucleate in this

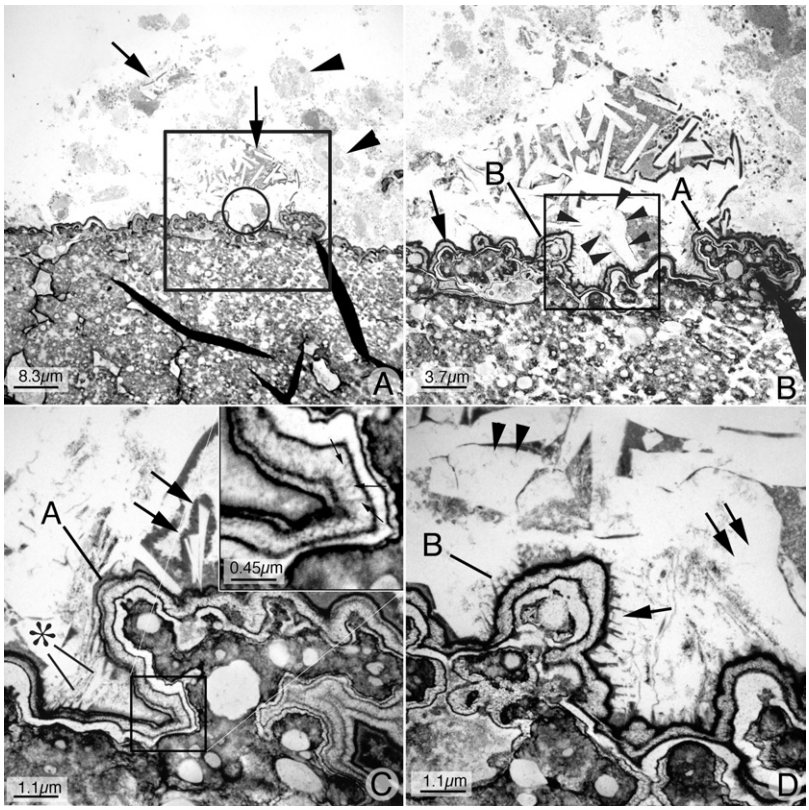

Figure 7. Transmission electron microscopy images of the tissue attachment site. (A) Randall's plaque in tissue at the attachment site (lower portion, transmission electron microscopy image) presents a sharply demarcated boundary to the original urine space (upper portion), which contains several rafts of large crystals (arrows) and cell debris (arrowheads). One raft lies closer to the surface (within the square) and a large crystal (within the circle) extends from the raft to the tissue surface. (B) At higher magnification of the square in A, many more crystals of this raft are seen to extend to and reach the plaque surface (within the square). A particularly large crystal within the circle of A is highlighted here by small arrowheads. The plaque boundary has the appearance of a multilayered ribbon (single arrow at left). (C) At higher magnification the plaque boundary has 9 separate layers (small square and square insert at upper right), in which 5 thin black organic lamina alternate with 4 white lamina. In the thickest of the white lamina one can see tiny thin spicules that run perpendicular to the surface and have the appearance of multiple voids that contained tightly packed crystals (small arrows, insert). Large numbers of small crystals are growing into the outer border of the ribbon (asterisk) and merge with more peripheral large crystals that are embedded in a homogeneous gray matrix in what was the urine space. Double arrows highlight a large in-growing crystal. (D) The region marked *B* reveals the same pattern of tiny crystals growing into the plaque border and merging with large crystals embedded in a homogeneous matrix and extending into the urine space. Double arrows mark a large crystal already highlighted by small arrowheads in B; its relationship to large numbers of smaller crystals that eventually merge into the plaque border (arrow) is apparent. Very large sharp-edged crystals in what was the urine space are surrounded by a homogeneous grey matrix (arrowheads). Magnification is as follows: (A) 1,200×, (B) 1,800×, (C) 8,800×, and (D) 8,800×. Reprinted with permission from Evan et al.[16]

urine matrix, the crystals themselves can attract molecules that have affinities for them, thereby creating the new stone.

UNIQUE CHARACTER OF ICSF PATHOLOGY VERSUS ALL OTHER FORMS TO DATE

What we have shown here has been found to date in no other type of stone-forming patient but the ICSF. Patients whose stones contain brushite (calcium monohydrogen phosphate) have plaque,[17] but their inner medullary collecting ducts (IMCDs) and ducts of Bellini (BD) often are plugged with apatite crystals; cell death and interstitial fibrosis are usual with deposits. Attached stones on plaque are not found. Patients with intestinal bypass for obesity and CaOx stones have no plaque; they have

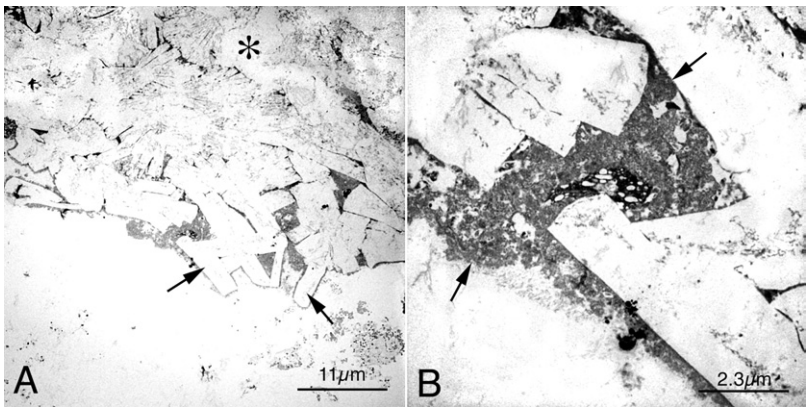

Figure 8. Transmission electron microscopy images of the stone attachment site. (A) Large lath-shaped crystals are seen embedded in a featureless gray matrix that closely resembles the rafts in Figure 7. (B) At higher magnification of the region at the arrow in A, the matrix appears coarsely granular and does not contain the characteristic round voids of Randall's plaque. Magnification is as follows: (A) 1,200×, and (B) 1,800×. Reprinted with permission from Evan et al.[16]

IMCD apatite plugging, as in brushite stones, although milder.[2] Patients with apatite stones and renal tubular acidosis resemble those with brushite disease except that the plugging and interstitial fibrosis are more diffuse.[18] Patients with cystinuria plug their BD with cystine, but also plug IMCDs with apatite.[19] In other words, ICSFs appear to be the special case, although the most commonly encountered one, in which stones form external to the kidney and by processes that do not involve the epithelial compartments.

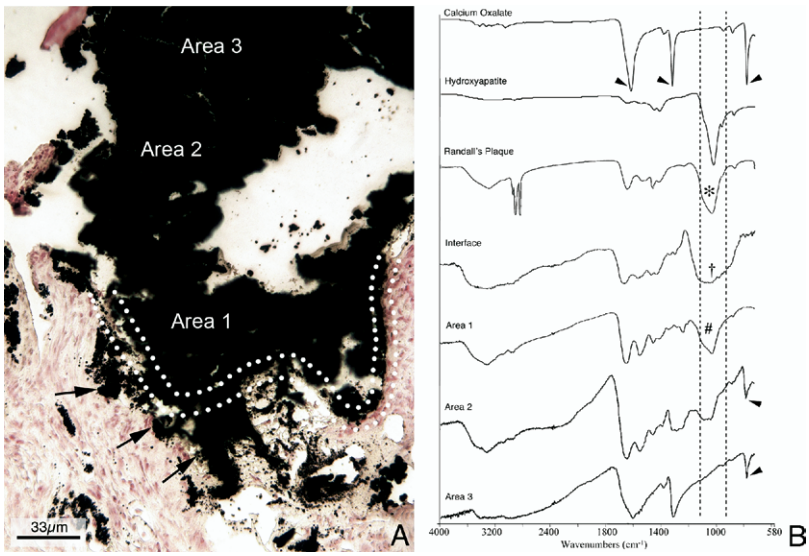

Figure 9. Light microscopic images of the stone–tissue interface and micro-FTIR analysis. (A) In the Yasue-stained section, kidney tissue (bottom) contains Randall's plaque accumulations (arrows) near the stone interface cross the interface and merge into the mineral of the attached stone (area 1). Stone mineral extends continuously from region 1 into the stone interior (areas 2 and 3). (B) Micro-FTIR analysis of the tissue section revealed the characteristic band for hydroxyapatite (asterisk) for the large mass of plaque (A, arrows). The interface itself (A, between white dotted lines) revealed a broadened band (B, †) characteristic of amorphous apatite. (A) Area 1 revealed the typical hydroxyapatite band (B, #). (A) In area 2 bands of hydroxyapatite and CaOx (B, arrowhead, tracing marked area 2) both were detected. (A) Finally, in area 3, toward the urine space border of the stone, μ-FTIR revealed only CaOx (B, arrowhead). Reprinted with permission from Evan et al.[16]

IMPLICATIONS FOR RESEARCH AND CLINICAL PRACTICE

Perhaps the most obvious remark is that renal pathology of stone formers will vary with even subtle clinical distinctions—brushite in CaOx stones, for example. So pathology without clinical detail is uninterruptible. The mechanisms producing plaque are crucial to understanding ICSFs, and are unknown. A true animal model would be invaluable. For clinicians, the ability to quantify plaque radiographically could prove very valuable in patient care because we do not know what one can do to prevent it, or even cause some regression. Urologists now can visualize the papillae routinely via flexible ureteroscopy using digital optics; when stones are seen on plaque, the patient is almost certainly an ICSF, and when IMCDs and BD are seen to be plugged the diagnosis must be otherwise. Conversion from CaOx to apatite or brushite indicates a parallel conversion from plaque and attachment to IMCDs and BD plugging with distinctive renal disease, so treatment efforts should be increased. How to avoid such conversion is not known.

REFERENCES

1. Coe FL, Evan A, Worcester E. Kidney stone disease. J Clin Invest. 2005;115:2598-608.
2. Evan AP, Lingeman JE, Coe FL, et al. Randall's plaque of patients with nephrolithiasis begins in basement membranes of thin loops of Henle. J Clin Invest. 2003;111:607-16.
3. Evan AP, Coe FL, Rittling SR, et al. Apatite plaque particles in inner medulla of kidneys of calcium oxalate stone formers: osteopontin localization. Kidney Int. 2005;68:145-54.
4. Evan AP, Bledsoe S, Worcester EM, et al. Renal inter-alpha-trypsin inhibitor heavy chain 3 increase in calcium oxalate stone-forming patients. Kidney Int. 2007;72:1503-11.
5. Asplin JR, Arsenault D, Parks JH, et al. Contribution of human uropontin to inhibition of calcium oxalate crystallization. Kidney Int. 1998;53:194-9.
6. Vernon HJ, Osborne C, Tzortzaki EG, et al. Aprt/Opn double knockout mice: osteopontin is a modifier of kidney stone disease severity. Kidney Int. 2005;68: 938-47.
7. Wesson JA, Johnson RJ, Mazzali M, et al. Osteopontin is a critical inhibitor of calcium oxalate crystal formation and retention in renal tubules. J Am Soc Nephrol. 2003;14:139-47.
8. Worcester EM, Beshensky AM. Osteopontin inhibits nucleation of calcium oxalate crystals. Ann N Y Acad Sci. 1995;760:375-7.
9. Atmani F, Khan SR. Role of urinary bikunin in the inhibition of calcium oxalate crystallization. J Am Soc Nephrol. 1999;10 Suppl 14:S385-8.
10. Atmani F, Glenton PA, Khan SR. Role of inter-alpha-inhibitor and its related proteins in experimentally induced calcium oxalate urolithiasis. Localization of proteins and expression of bikunin gene in the rat kidney. Urol Res. 1999;27:63-7.
11. Iida S, Peck AB, Byer KJ, Khan SR. Expression of bikunin mRNA in renal epithelial cells after oxalate exposure. J Urol. 1999;162:1480-6.
12. Kuo RL, Lingeman JE, Evan AP, et al. Urine calcium and volume predict coverage of renal papilla by Randall's plaque. Kidney Int. 2003;64:2150-4.
13. Daudon M, Traxer O, Jungers P, et al. Stone morphology suggestive of Randall's plaque. In: Evan AP, Lingeman JE, Williams JC Jr, editors. Proceedings of the First Annual International Urolithiasis Research Symposium. AIP Conference Proceedings. Melville, NY: American Institute of Physics; 2007. p. 26-34.
14. Matlaga BR, Miller NL, Terry C, et al. The pathogenesis of calyceal diverticular calculi. Urol Res. 2007;35: 35-40.
15. Kim SC, Matlaga BR, Tinmouth WW, et al. In vitro assessment of a novel dual probe ultrasonic intracorporeal lithotriptor. J Urol. 2007;177:1363-5.
16. Evan AP, Coe FL, Lingeman JE, et al. Mechanism of formation of human calcium oxalate renal stones on Randall's plaque. Anat Rec. 2007;290:1315-23.
17. Evan AP, Lingeman JE, Coe FL, et al. Crystal-associated nephropathy in patients with brushite nephrolithiasis. Kidney Int. 2005;67:576-91.
18. Evan AP, Lingeman J, Coe F, et al. Renal histopathology of stone-forming patients with distal renal tubular acidosis. Kidney Int. 2007;71:795-801.
19. Evan AP, Coe FL, Lingeman JE, et al. Renal crystal deposits and histopathology in patients with cystine stones. Kidney Int. 2006;69:2227-35.